Interaction Notes
Note 631

November 7, 2019

HEMP Response Estimates of Buried Cables within a Communications Facility

Dr. F. M. Tesche, EM Consultant (Retired), USA

Dr. D. V. Giri, Pro-Tech, Wellesley, MA
Dept. of ECE, University of New Mexico, Albuquerque, NM, USA

and

Dr. Armin Kälin, formerly with armasuisse, now with EMProtec GmbH, Switzerland

Abstract

This note estimates the responses of four different types of shielded cables to high - altitude nuclear electromagnetic pulse (HEMP) environments. The same cable geometry and shield parameters used in a previous study of a direct-strike lightning excitation are used here, thereby permitting a comparison of the lightning and HEMP responses.

1. Introduction

In an earlier report [1], a parametric study of overhead and buried cables excited by a nuclear electromagnetic pulse (NEMP) was described. This study involved examining various line lengths and developing estimates of the response statistics for the *external* currents and voltages induced along the line. Parameters that were varied randomly included the angles of incidence ϕ, ψ and the polarization angle of the excitation field, γ. Deterministic parameters included the cable length, the height (or burial depth) of the cable, the earth conductivity, and the impedance termination conditions. Various cable responses were developed for three different HEMP environments, and the resulting data were summarized statistically.

In realistic system problems, however, estimates of the exterior cable responses may not be sufficient for developing hardening requirements for internal equipment. For example, the equipment within a facility rarely experiences the high levels of the external stress on the system. Additional shielding provided by the first topological shield within the system can serve to significantly reduce this stress [2], and this effect must be taken into account in any calculation.

In another accompanying note the response of a communications system to a direct lightning strike has been examined [3]. As diagramed in Figure 1, this facility consists of two shielded enclosures connected by a length of buried cable or conduit through which electrical signal or power wires pass. The external current induced on the buried cable shield (which was estimated in [1]) is able to diffuse through the shield and induce internal voltages on the inner wires. It is this voltage that is potentially damaging to the internal equipment.

In the present note, the facility shown in Figure 1 is again considered, but with the excitation now being an incident transient plane wave representing a HEMP. Because there is a need to coordinate the HEMP and lightning protection requirements, the data generated in this study can be combined with that of [3] to develop specific protection guidelines for this and similar systems.

As in the previous HEMP coupling studies, we will take a statistical view in developing the estimates of the system responses. In addition to simply letting the angles of incidence and polarization vary randomly, we also let the cable length, burial depth and earth conductivity vary randomly within various pre-set limits. As a result, we are able to see quite clearly the expected probability distributions for the various responses.

Specifically, we will be examining the behavior of the external shield current (similar to that computed in [1] for the buried cables), and the internal voltage induced on the signal or power cables located within the shielded cable.

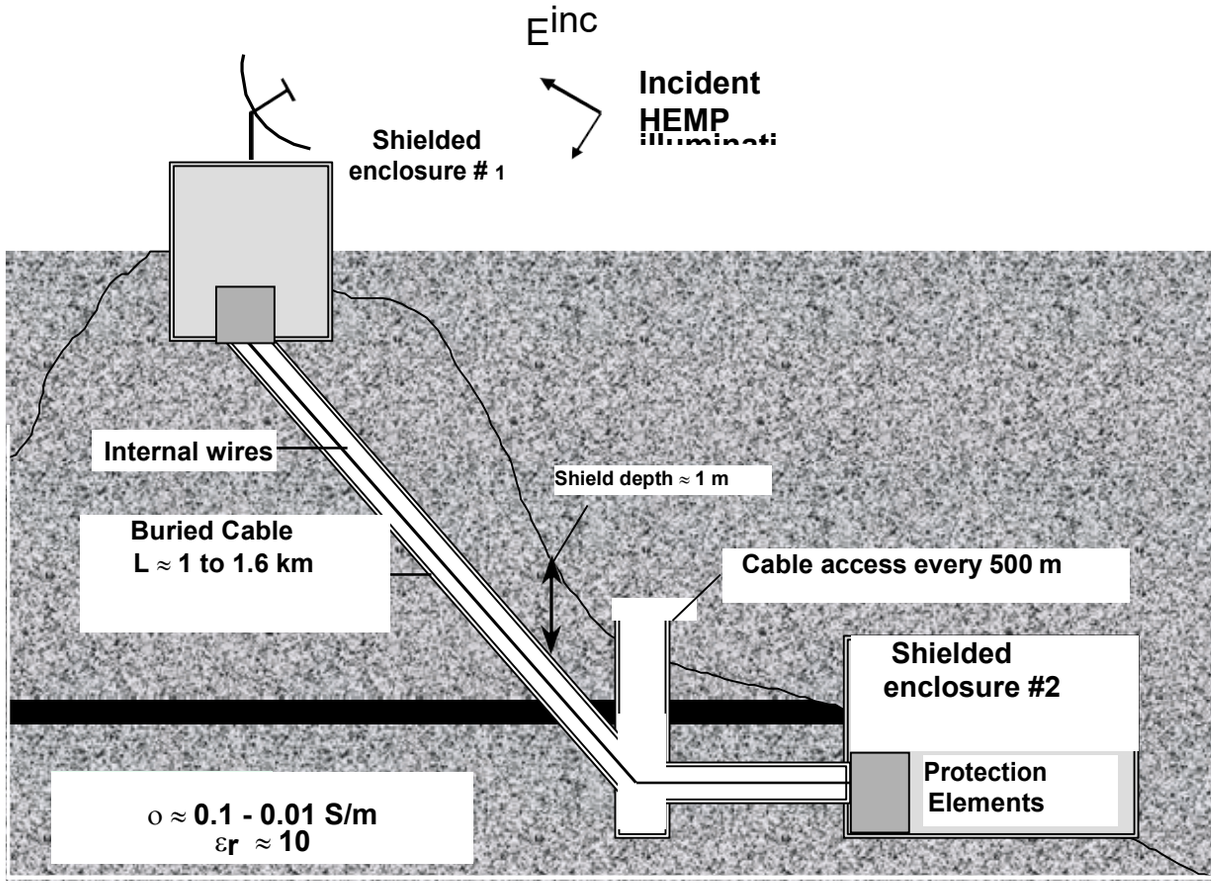

Figure 1. Illustration of the communications facility with buried cables, excited by an incident HEMP.

2. The HEMP Environment

For these calculations, the same three HEMP environments defined in [1] are used. These are the Bell Laboratory waveform [4], the IEC HEMP waveform [5], and the German VG Standard waveform [6]. These transient fields are assumed to be plane waves, described by a vertical angle of incidence with respect to the ground, ψ , and an azimuthal angle ϕ. In addition to these angles, there is a polarization angle, γ, which is the angle between the E-field vector and the vertical plane of incidence. These angles are illustrated in Figure 2.

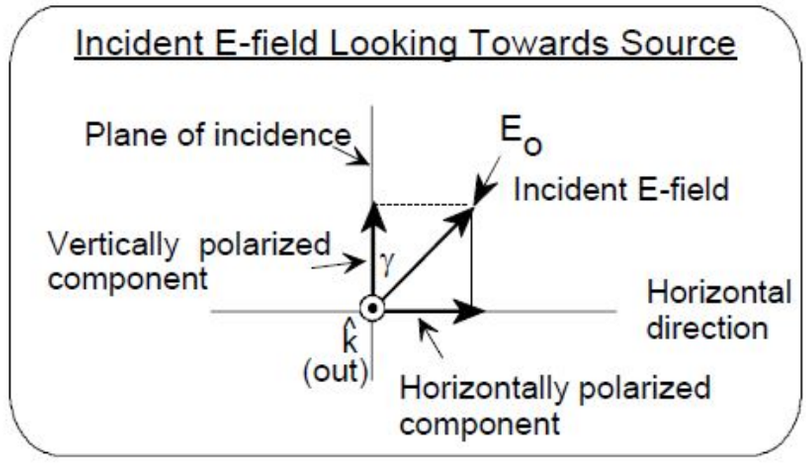

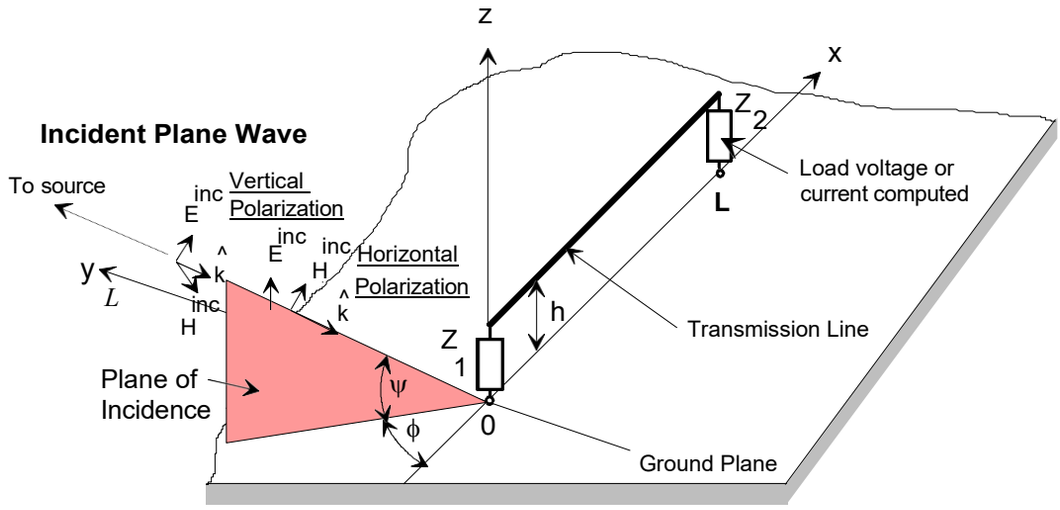

Figure 2. Definition of the HEMP excitation.

Each of the three transient environments is represented by a simple double exponential waveform of the form

$$E^{inc}(t) = E_o \Gamma \left(e^{-\alpha t} - e^{-\beta t} \right), \tag{1}$$

where α and β are time constants for the waveforms, E_o is the peak amplitude of the waveform and Γ is a normalizing constant to ensure that the quantity $\Gamma\left(e^{-\alpha t} - e^{-\beta t}\right)$, is unity at $t = t$ is unity at $t = t_{peak}$. Values for these parameters are provided in Table 1, and the waveforms are illustrated in Figure 3.

Table 1. Waveform parameters for the HEMP waveforms.

Waveform	E_0 (kV/m)	α (1/s)	β (1/s)	ρ
Bell Labs	50	4.0×10^6	4.76×10^8	1.05
IEC	50	4.0×10^7	6.0×10^8	1.30
VG Standard	65	3.22×10^7	2.07×10^9	1.08

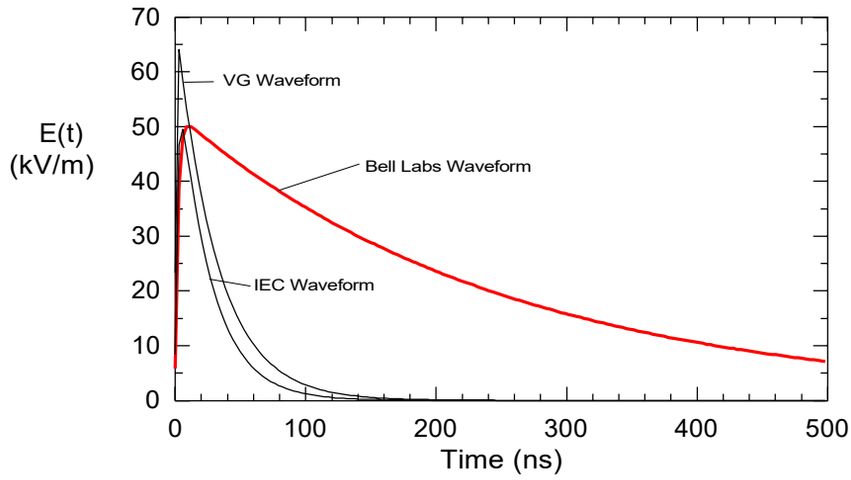

Figure 3. Plot of the HEMP waveforms used for estimating cable responses.

3. The Cable Coupling Model

The calculation of the internal voltage responses on the shielded cable in the system of Figure 1 can be accomplished through the use of a suitable cable coupling model described in [7]. This model is illustrated in Figure 4, in which a two-region transmission line problem is seen. There is the external transmission line, consisting of the buried cable shield and termination resistances R_1 and R_3 at each end of the line. The incident HEMP field induces a current on the cable shield, $I(x)$, and this must be determined using a suitable transmission line model.

Using the *transfer impedance* concept for the internal wire excitation [8], a set of distributed voltage source $V'_s(\omega)$ on the internal wire within the shield is produced by the external shield current. This is given by the expression

$$V_s'(\omega) = Z_t'(\omega) I(x) \quad . \tag{1}$$

$Z'_t(\omega)$ is a frequency-dependent transfer impedance of the shield and it depends on both the shield geometry and the electrical properties of the shield material.

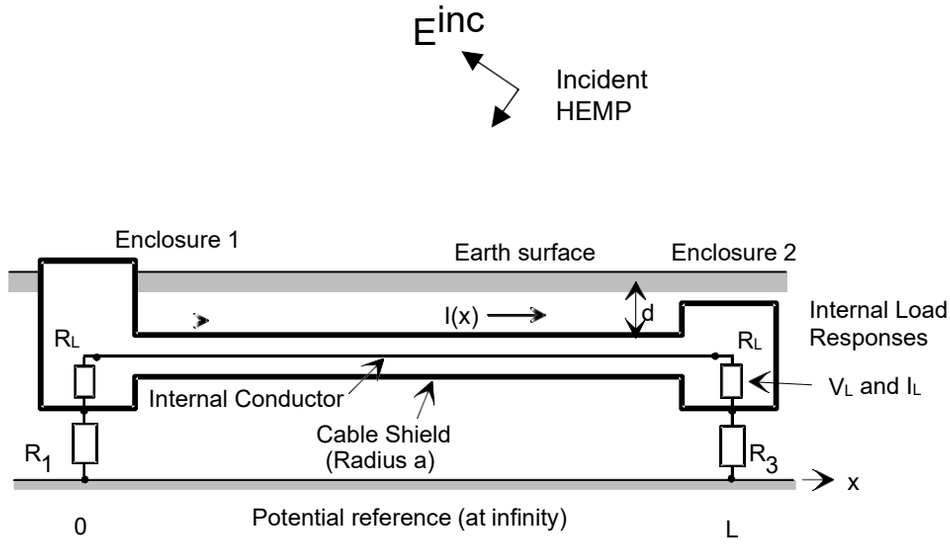

Figure 4. Detailed cable model of the shield and internal wire excited by a HEMP.

The expressions for computing the external and internal responses of the shielded cable in Figure 4 are given in Chapter 9 of [7]. Because the cable shield is buried, a slight simplification results in the determination of the excitation function of external problem. Only the tangential E-field of Eq.(9.66b) needs to be considered, with the field tangential to the line being given by the E-field in the earth at the depth of the line (see Eq.(8.81) in [7] for the appropriate expression.)

Moreover, in the present analysis, we will assume that the internal line is appropriately matched to the characteristic impedance of the inner coaxial region. This eliminates the internal resonances within the shielded line and simplifies the results. This matched load response is not a worst-case response, however. The worst case voltage response occurs when the internal load is open circuited, and this may be estimated as twice the matched load response. Similarly, the worst case response for the load current occurs when the inner line is terminated in a short circuit, and this response is approximately twice the current of the matched load. Additional details of the calculational model used for this buried line is provided in [7].

4. Computed Response Estimates

Using the buried coaxial line model, Monte Carlo calculations were conducted, in which the line parameters varied randomly and the line responses were noted. The line parameters varied in this study included:

- Line length L – from 5 m to 1000 m
- Depth of the line d – from 0.1 m to 3 m
- Earth conductivity σ – from 0.001 to 0.1 S/m
- Polarization angle γ – from 0 to 360°
- Azimuthal angle of incidence ϕ – from 0 to 360°
- Vertical angle of incidence ψ – from 0 to 90°

Each of the above variables was assumed to have a uniform probability distribution over its specified range, with the exception of the angle ψ , which had a distribution that provided a uniform probability density of the solid angle $d\Omega = \cos\psi \, d\psi \, d\phi$.

In addition to these parameters, the footing resistances R_1 and R_3 of the external transmission line model were assumed to be fixed at a constant value of 5Ω, and the relative dielectric constant of the soil was fixed at $\varepsilon_r = 10$.

The cables treated in this report are the same cables examined for the lightning study of ref. [3]. Table 2 of that reference provides the necessary description and electrical data for these cables.

4.1 External Shield Current Responses

For an example of the external cable current responses induced by the HEMP environment, the version 3 Cr-Ni-Steel cable was considered. This cable has an average diameter of 8.4 cm, and due to its poor conductivity, it provided the worst-case shielding of the internal wires. However, the external current is not expected to be highly dependent on the shield conductivity, so its responses are typical of those for the rest of the cables.

Figure 5 presents the cumulative probability distribution (CPD) for the peak value of the external shield current of the version 3 buried cable for HEMP excitation. These curves have been obtained from 1000 Monte Carlo calculations with randomly varying parameters. Responses for the Bell Laboratory waveform, the IEC waveform, and the German VG waveform are shown. Notice that upper bound responses (i.e., the worst-case responses) are in general agreement with those provided for the buried cables in Table 4 of ref. [1].

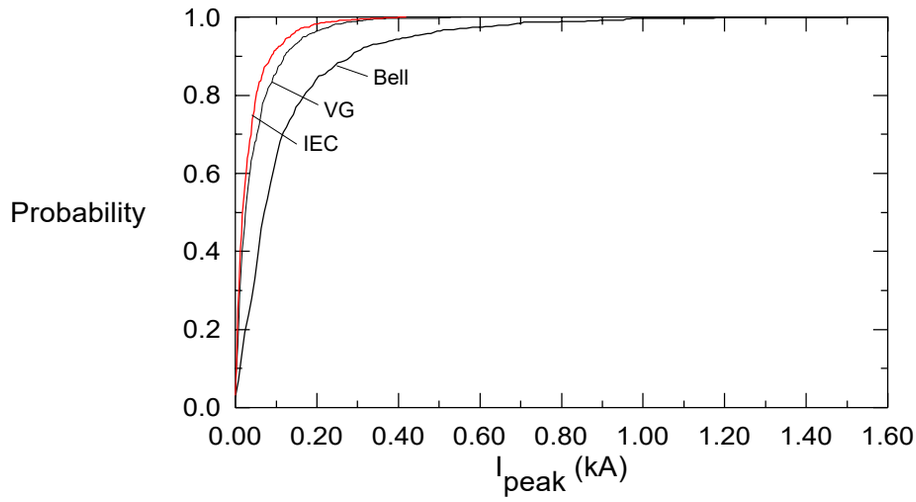

Figure 5. Cumulative probability distribution for the peak external shield current of the buried cable for HEMP excitation.

For the same cable, Figure 6 plots the CPD for the peak rate of rise of the external shield current for the three HEMP excitations. Notice that there is not much of a difference between the three environments, due to the fact that the lossy earth severely attenuates the fast-rise portions of waveforms. The statistics of the 50% fall times are different, however, as

noted in Figure 7. Here the Bell Laboratory waveform provides a much longer external cable current response.

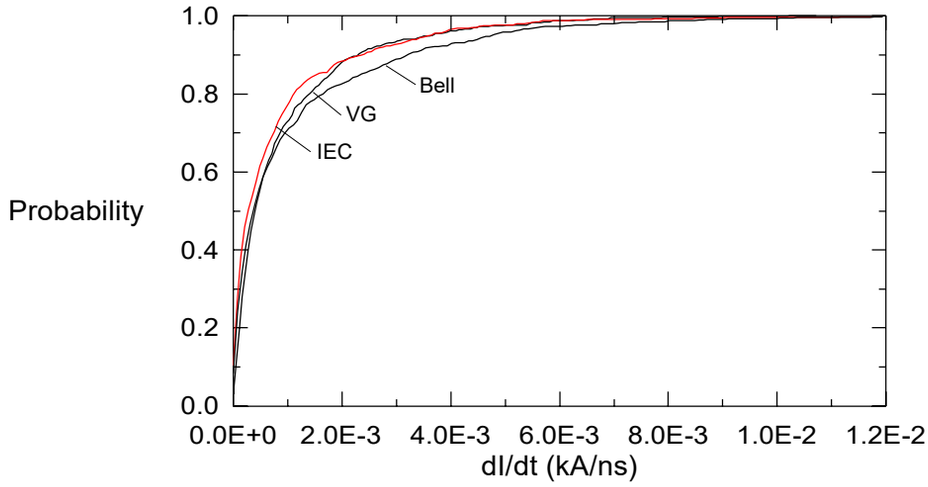

Figure 6. CPD for the peak rate of rise of the external shield current of the buried cable for HEMP excitation.

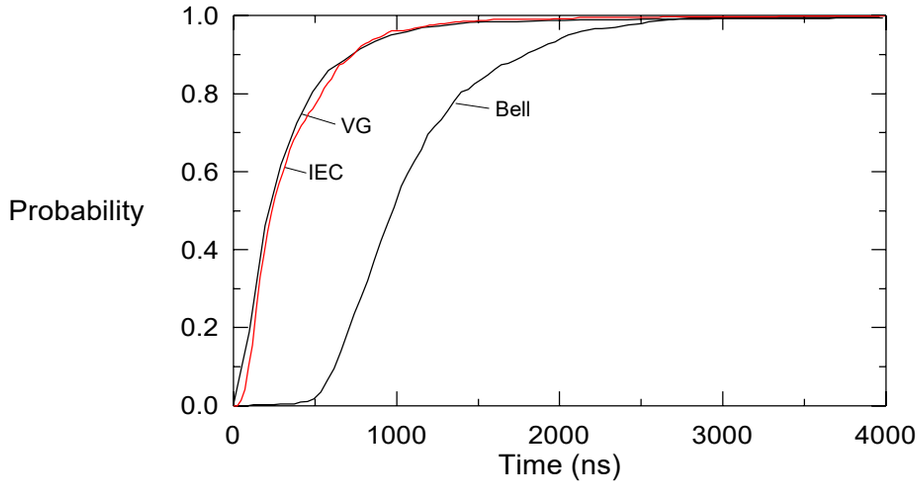

Figure 7. CPD for the fall-times of the external shield current of the buried cable for HEMP excitation.

These external current responses can be summarized in terms of the same "severity levels" that have been used for the other environments. Tables 2 - 4 provide the summaries for the peak shield current, the peak current derivative and the fall time. In these tables, the data in the 5% column, for example, indicates that only 5% of the cases will be expected to have a response *less* than the value in the table.

Table 2. Peak shield current (in kA) for different severity levels.

Environment	5%	10%	50%	90%	95%
Bell Labs	7.86E-03	1.57E-02	7.07E-02	0.283	0.432
IEC	2.10E-03	2.10E-03	1.89E-02	8.83E-02	0.134
VG	2.78E-03	5.56E-03	2.78E-02	0.122	0.167

Table 3. Peak shield current derivative (in kA/ns) for different severity levels.

Environment	5%	10%	50%	90%	95%
Bell Labs	5.39E-05	5.39E-05	4.31E-04	2.32E-03	3.66E-03
IEC	6.86E-05	6.86E-05	2.74E-04	2.40E-03	3.63E-03
VG	7.86E-05	7.86E-05	3.93E-04	3.22E-03	4.79E-03

Table 4. Shield current fall-time (in μs) for different severity levels

Environment	5%	10%	50%	90%	95%
Bell Labs	0.57	0.65	0.98	1.81	2.05
IEC	0.09	0.09	0.25	0.74	0.92
VG	0.10	0.10	0.29	0.77	0.97

4.2 Internal Voltage Responses

The HEMP-induced voltage responses inside the shielded cable have been computed for each of the four cable shield types described in ref.[3]. The results are summarized in this section.

4.2.1 Cable shield version 1

The version 1 cable was seen to provide the best protection against the lightning excitation, and it is expected that this will also be the case for the HEMP environments. Figure 8 plots the calculated CPD of the peak internal load voltage for the version 1 cable shield for the three different HEMP excitations. It is clear that the Bell Laboratory pulse provides the largest response of the three environments, but that the maximum voltage responses are rather small due to the excellent shielding properties of the cable.

Similarly, the CPD for the rate of rise of internal load voltage for the version 1 cable shield is shown in Figure 9.

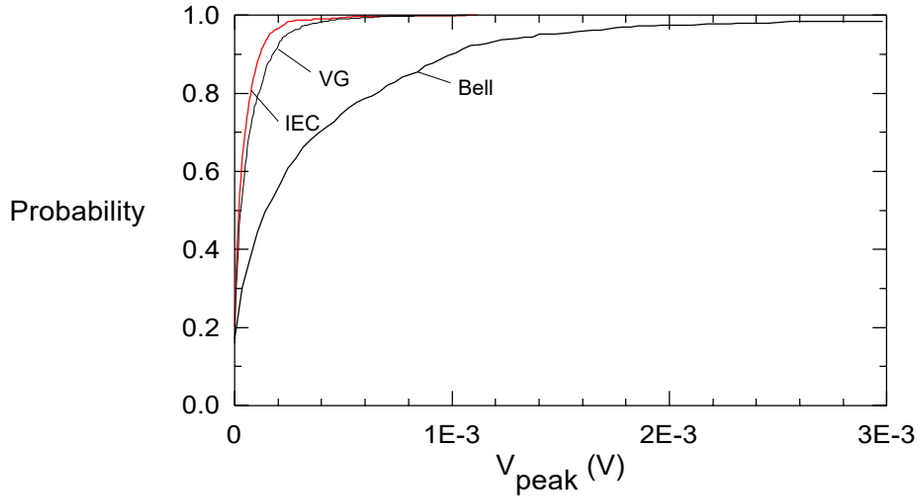

Figure 8. CPD of the peak internal load voltage for the version 1 cable shield for HEMP excitation.

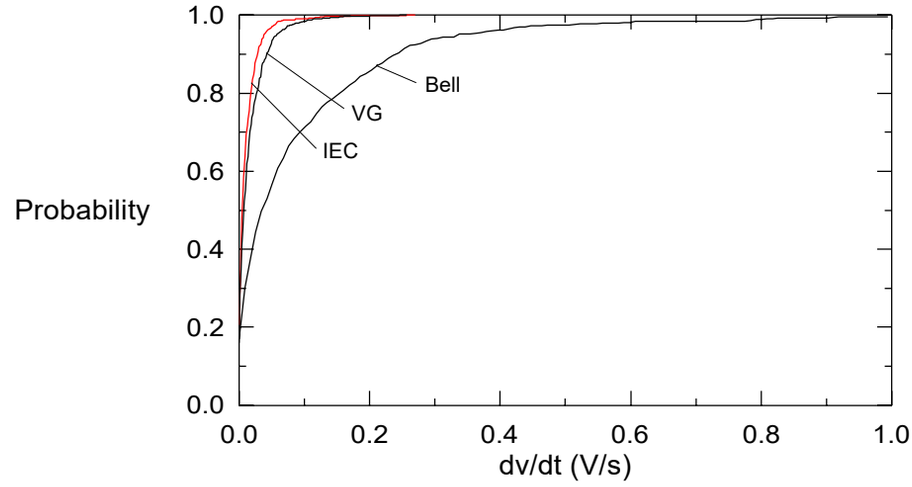

Figure 9. CPD of the internal load voltage rate of rise for the version 1 cable shield for HEMP excitation.

Figure 10 presents the CPD for the voltage waveform 50% fall time for the various HEMP environments. This is an interesting curve, in that it is the same for all environments, and it appears like a step function. This implies that the fall time is *independent* of the external excitation for this particular shield and is basically given by the field diffusion time through the shield.

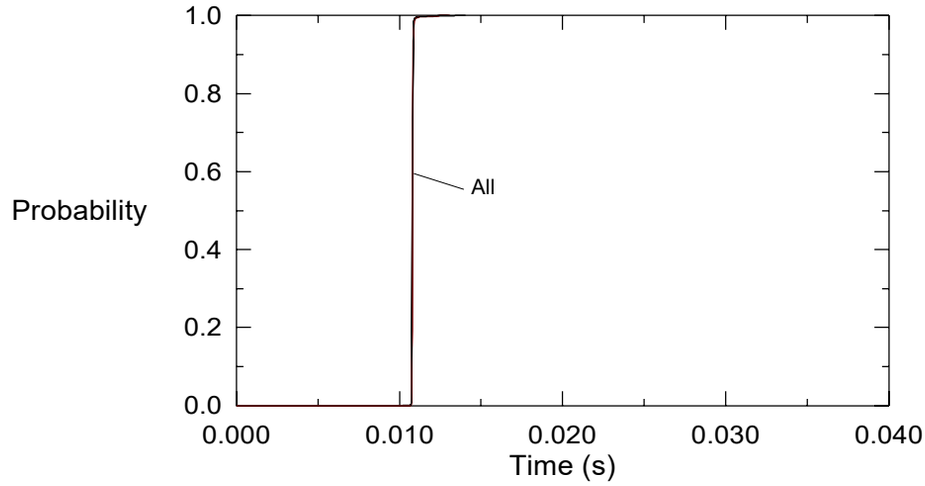

Figure 10. CPD of the internal load voltage fall time for the version 1 cable shield for HEMP excitation.

While the cumulative probability distributions in the previous curves adequately describe the responses, it is possible to summarize these results by using the five different severity levels used previously to describe the shield current levels. Table 5 presents the data for the peak internal wire voltage (in V) for the different severity levels for this shield. Table 6 presents the maximum time derivative of the internal wire voltage (in V/s), and Table 7 presents the 50% fall times (in seconds).

Table 5. Peak internal wire voltage (in V) for different severity levels for shield version 1.

Environment	5%	10%	50%	90%	95%
Bell Labs	3.50E-05	3.50E-05	1.75E-04	1.01E-03	1.40E-03
IEC	5.62E-06	5.62E-06	2.24E-05	1.18E-04	1.63E-04
VG	5.39E-06	5.39E-06	3.23E-05	1.77E-04	2.42E-04

Table 6. Maximum time derivative of the internal wire voltage (in V/s) for different severity levels for shield version 1.

Environment	5%	10%	50%	90%	95%
Bell Labs	8.42E-3	8.42E-3	4.21E-2	0.24	0.34
IEC	1.35E-3	1.35E-3	5.40E-3	2.83E-2	3.78E-2
VG	1.29E-3	1.29E-3	7.75E-3	4.26E-2	5.81E-2

Table 7. Fall time of the internal wire voltage (in s) for different severity levels for shield version 1.

Environment	5%	10%	50%	90%	95%
Bell Labs	0.011	0.011	0.011	0.011	0.011
IEC	0.011	0.011	0.011	0.011	0.011
VG	0.011	0.011	0.011	0.011	0.011

4.2.2 Cable shield version 2

Similar results are presented in this section for the version 2 cable shield. Figure 11 illustrates the CPDs for the peak voltage of the internal wire response, Figure 12 presents the data for the voltage derivative, and Figure 13 shows the CPDs for the 50% fall times for this shield. The corresponding data for five severity levels are presented in Table 8, Table 9 and Table 10.

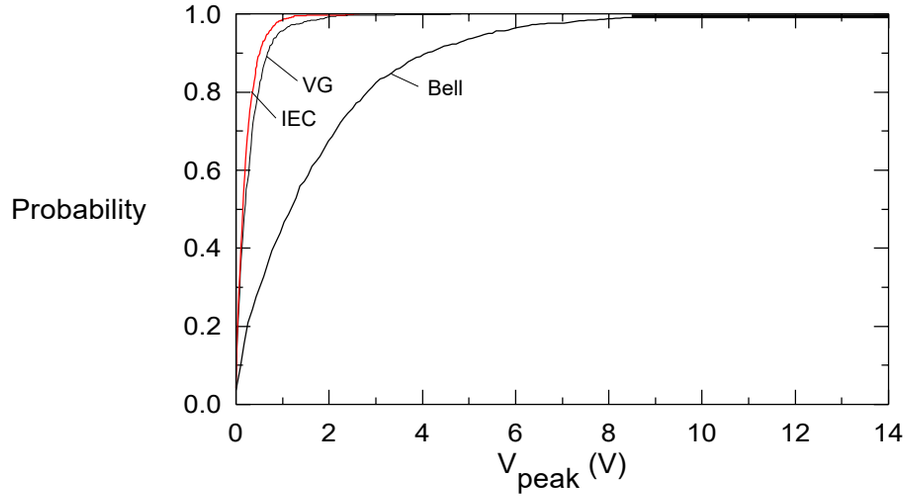

Figure 11. CPD of the peak internal load voltage for the version 2 cable shield for HEMP excitation.

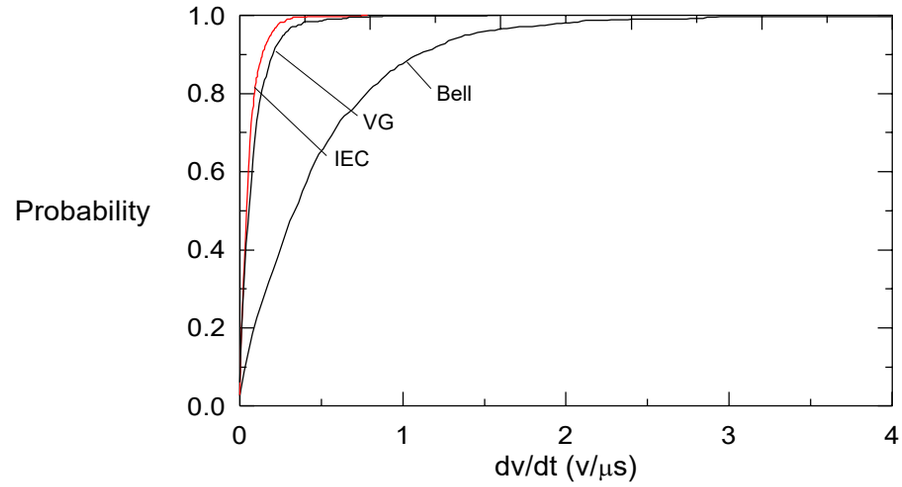

Figure 12. CPD of the internal load voltage rate of rise for the version 2 cable shield for HEMP excitation.

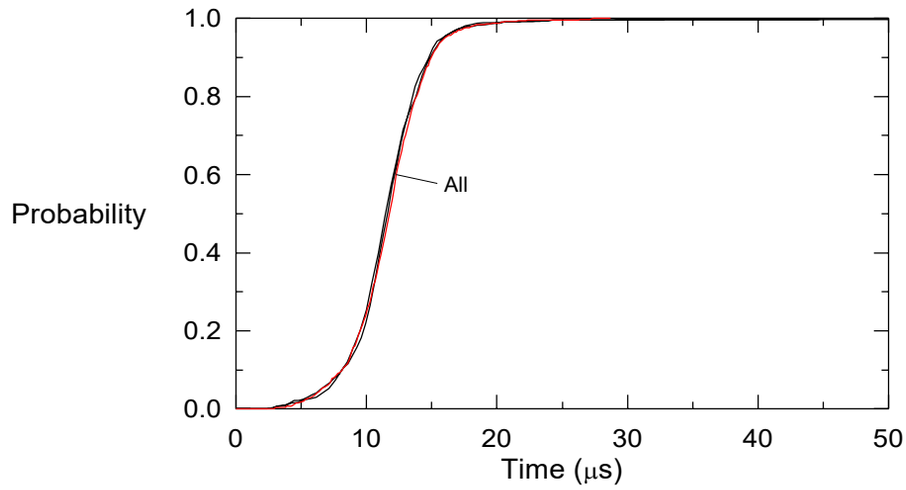

Figure 13. CPD of the internal load voltage fall time for the version 2 cable shield for HEMP excitation.

Table 8. Peak internal wire voltage (in V) for different severity levels for shield version 2.

Environment	5%	10%	50%	90%	95%
Bell Labs	8.58E-02	0.17	1.20	4.12	5.40
IEC	1.32E-02	1.32E-02	0.14	0.50	0.69
VG	2.42E-02	2.42E-02	0.19	0.68	0.89

Table 9. Maximum time derivative of the internal wire voltage (in V/μs) for different severity levels for shield version 2.

Environment	5%	10%	50%	90%	95%
Bell Labs	0.03	0.05	0.36	1.10	1.38
IEC	0.004	0.008	0.04	0.14	0.19
VG	0.008	0.008	0.06	0.21	0.27

Table 10. Fall time of the internal wire voltage (in ms) for different severity levels for shield version 2.

Environment	5%	10%	50%	90%	95%
Bell Labs	7.11	8.53	11.85	15.17	16.12
IEC	7.11	8.53	11.85	15.17	16.12
VG	7.11	8.53	11.85	15.17	16.12

4.2.3 Cable shield version 3

The version 3 cable shield was seen to provide the worst protection against the lightning threat to the system, due to its relatively low conductivity and the fact that it does not provide magnetic shielding. Applying the HEMP coupling model to this shield yields similar results for the three HEMP environments. Figure 14, Figure 15 and Figure 16 present the three CPDs used to describe the internal voltage responses in this case, and the numerical data are summarized in Table 11, Table 12 and Table 13.

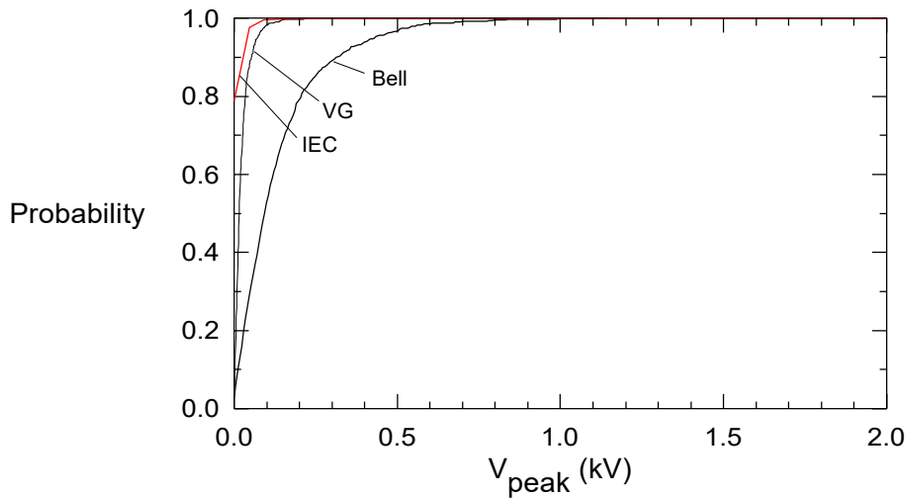

Figure 14. CPD of the peak internal load voltage for the version 3 cable shield for HEMP excitation.

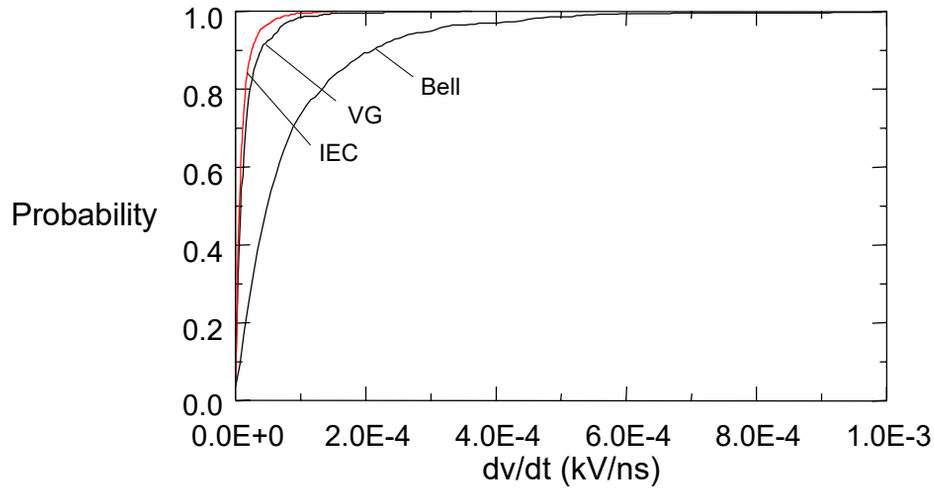

Figure 15. CPD of the internal load voltage rate of rise for the version 3 cable shield for HEMP excitation.

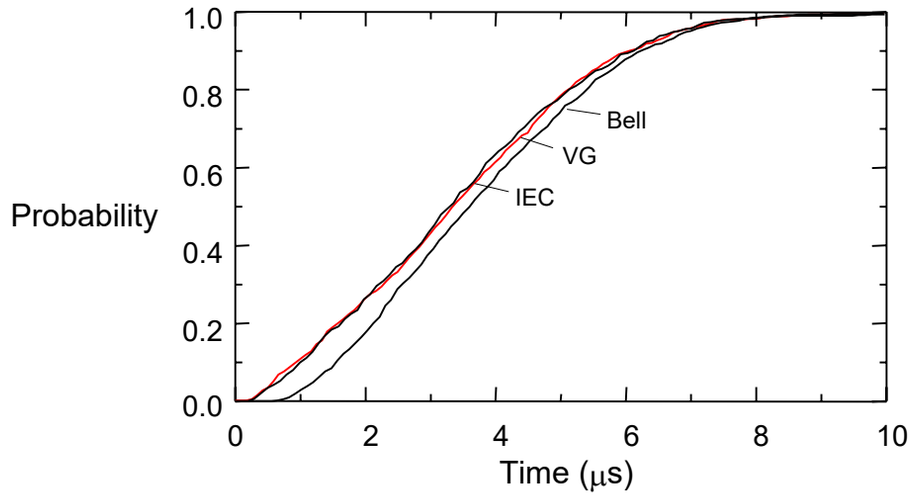

Figure 16. CPD of the internal load voltage fall time for the version 4 cable shield for HEMP excitation.

Table 11. Peak internal wire voltage (in V)
for different severity levels for shield version 3.

Environment	5%	10%	50%	90%	95%
Bell Labs	10.1	10.1	101	284	417
IEC	3.1	3.1	12.5	37.7	50.3
VG	1.8	1.8	16.2	53.9	75.5

Table 12. Maximum time derivative of the internal wire voltage (in kV/ns) for different severity levels for shield version 3.

Environment	5%	10%	50%	90%	95%
Bell Labs	6.80E-06	1.36E-05	5.44E-05	2.10E-04	3.06E-04
IEC	7.79E-07	7.79E-07	6.23E-06	2.49E-05	3.74E-05
VG	1.82E-06	1.82E-06	9.12E-06	4.01E-05	6.56E-05

Table 13. Fall time of the internal wire voltage (in μs) for different severity levels for shield version 3.

Environment	5%	10%	50%	90%	95%
Bell Labs	1.290	1.566	3.593	6.265	7.003
IEC	0.581	0.996	3.405	6.063	6.810
VG	0.691	1.085	3.356	6.120	6.811

4.2.4 Cable shield version 4

Similar results are obtained for the version 4 cable shield. Figure 17 illustrates the CPDs for the peak voltage of the internal wire response, Figure 18 presents the data for the voltage derivative, and Figure 19 shows the CPDs for the 50% fall times for this shield. The corresponding data for five severity levels are presented in Table 14, Table 15 and Table 16.

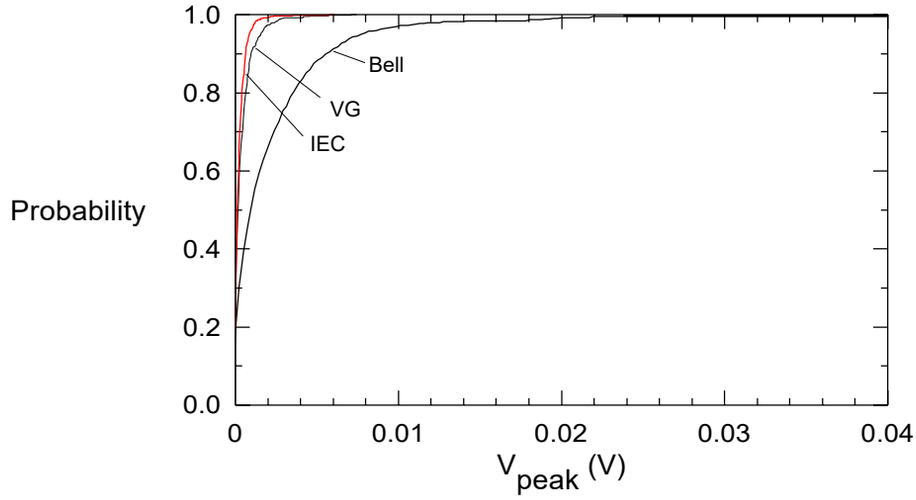

Figure 17. CPD of the peak internal load voltage for the version 4 cable shield for HEMP excitation.

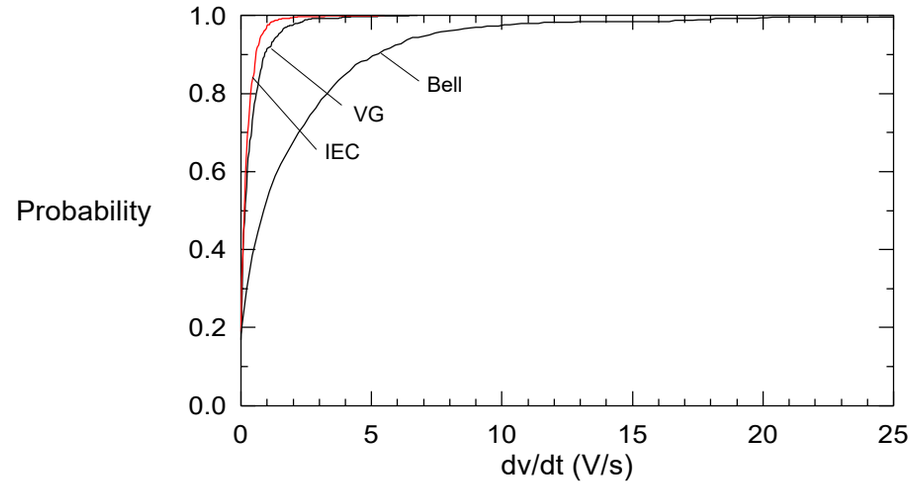

Figure 18. CPD of the internal load voltage rate of rise for the version 4 cable shield for HEMP excitation.

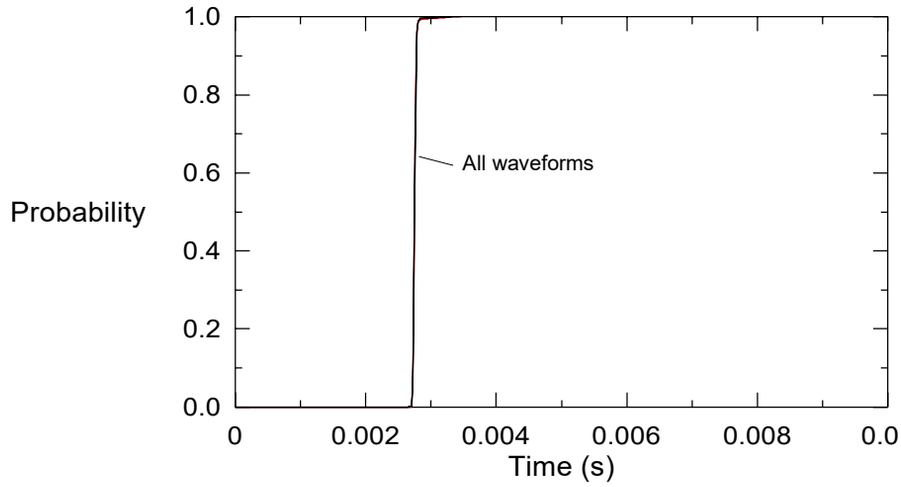

Figure 19. CPD of the internal load voltage fall time for the version 4 cable shield for HEMP excitation.

Table 14. Peak internal wire voltage (in V) for different severity levels for shield version 4.

Environment	5%	10%	50%	90%	95%
Bell Labs	2.40E-04	2.40E-04	9.63E-04	5.53E-03	7.70E-03
IEC	3.04E-05	3.04E-05	1.52E-04	6.38E-04	8.51E-04
VG	3.74E-06	3.74E-06	1.87E-05	9.73E-05	1.57E-04

Table 15. Maximum time derivative of the internal wire voltage (in V/s) for different severity levels for shield version 4

Environment	5%	10%	50%	90%	95%
Bell Labs	0.22	0.22	0.87	5.25	7.22
IEC	2.76-E2	2.76E-2	0.14	0.58	0.80
VG	3.39E-2	3.39E-2	0.17	0.92	1.42

Table 16. Fall time of the internal wire voltage 4 (in s) for different severity levels for shield version.

Environment	5%	10%	50%	90%	95%
Bell Labs	2.73E-3	2.73E-3	2.74E-3	2.78E-3	2.78E-3
IEC	2.73E-3	2.73E-3	2.74E-3	2.78E-3	2.78E-3
VG	2.73E-3	2.73E-3	2.74E-3	2.78E-3	2.78E-3

5. Summary

It is useful to compare the HEMP responses of the shielded cable estimated in this report with the lightning responses discussed earlier in ref.[3]. In this previous report, the lightning response of a 1 km buried line was provided for the same cable shields considered here. This previous calculation used an assumed 90% lightning stress, with a direct-strike current of 50 kA being applied directly to the cable building.

In the statistical description of the line responses presented in the present report, the most important physical parameters were permitted to vary over a specified range of values. These parameters included the following:

- Line length L
- Depth of the line d
- Earth conductivity σ
- Polarization angle γ
- Azimuthal angle of incidence ϕ
- Vertical angle of incidence ψ

To compare the lightning and HEMP responses, the statistical HEMP calculations described earlier in this report were re-done, with the line length *fixed* at 1 km. In this manner, the line length variations are removed from the solution and the line is similar to that used in the lightning study. Moreover, to have a consistent environmental level for the comparisons, the 90% response levels of the HEMP response probability distributions are used to compare with the responses to the 90% lightning environment. In this manner, both the lightning and the HEMP responses can be considered as "reasonable" upper bounds.

Table 17 presents a summary of the 90th percentile peak voltage, rate of rise and 50% fall time for the lightning and HEMP environments, for each of the four shield versions. In this table, all of the units are the same, with the peak voltage being in volts, the rate of rise beingin volts/sec, and the 50% fall time being in seconds.

These comparisons are also presented visually in Figure 20 through Figure 25. The 90% peak voltage response for the internal wires is shown in Figure 20 as a function of the EM environment, with the shield version as a parameter. The same data is illustrated in Figure 21, with the voltage being plotted as a function of the shield type, with the EM environment as a parameter. Similarly, the 90% values for the maximum waveform derivative dv/dt are presented in Figure 22 and Figure 23, and the waveform fall times are indicated in Figure 24 and Figure 25.

From these summary plots, it is obvious that the lightning strike provides the maximum response in the system. This is due to the relatively large amount of current flowing on the cable shield, together with the fact that the current waveform has less high frequency content that do the HEMP-induced currents. Moreover, it is evident that the version 3 shield provides the least protection of all of the shields, with the version 1 shield being the best.

Table 17. Summary of the 90th percentile peak voltage, rate of rise and 50% fall time for the lightning and HEMP environments using the four shield versions. (Line length = 1 km.)

Environment	Shield Type	Peak Voltage (V)	Rise Time (V/s)	50% Fall Time (s)
Lightning	Version 1	1.00×10^{2}	5.0×10^{3}	6.3×10^{-3}
	Version 2	2.00×10^{3}	1.0×10^{9}	6.1×10^{-5}
	Version 3	7.00×10^{4}	3.5×10^{10}	6.1×10^{-5}
	Version 4	2.00×10^{2}	6.5×10^{4}	9.9×10^{-3}
HEMP (Bell Laboratory)	Version 1	2.40×10^{-3}	5.77×10^{-1}	1.08×10^{-2}
	Version 2	6.63×10^{0}	1.52×10^{6}	1.77×10^{-5}
	Version 3	4.45×10^{2}	1.55×10^{8}	8.14×10^{-6}
	Version 4	1.32×10^{-2}	1.19×10^{1}	2.79×10^{-3}
HEMP (IEC)	Version 1	2.49×10^{-4}	5.98×10^{-2}	1.08×10^{-2}
	Version 2	7.89×10^{-1}	1.87×10^{5}	1.72×10^{-5}
	Version 3	4.04×10^{2}	1.93×10^{7}	7.80×10^{-6}
	Version 4	1.40×10^{-3}	1.29×10^{0}	2.81×10^{-3}
HEMP (VG)	Version 1	3.93×10^{-4}	9.45×10^{-2}	1.08×10^{-2}
	Version 2	1.08×10^{0}	2.66×10^{5}	1.72×10^{-5}
	Version 3	7.61×10^{1}	2.67×10^{7}	8.20×10^{-6}
	Version 4	2.13×10^{-3}	1.93×10^{0}	2.81×10^{-3}

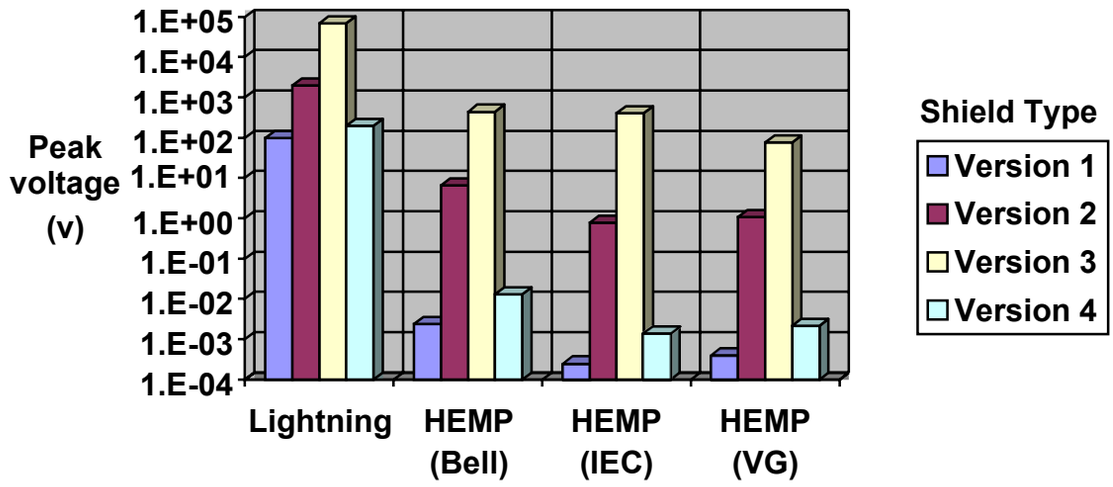

Figure 20. Plot of the 90% peak voltage responses of the internal shielded wires as a function of the EM environment. (Line length = 1 km.)

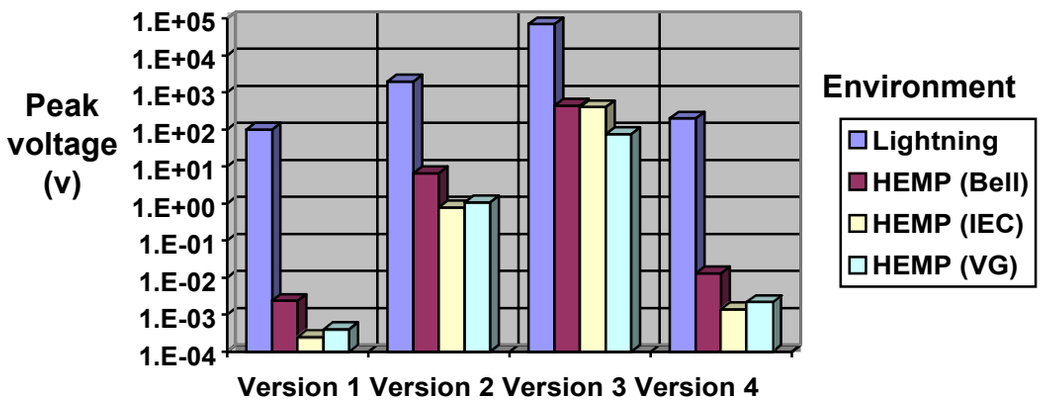

Figure 21. Plot of the 90% peak voltage responses of the internal shielded wires as a function of the cable shield version. (Line length = 1 km.)

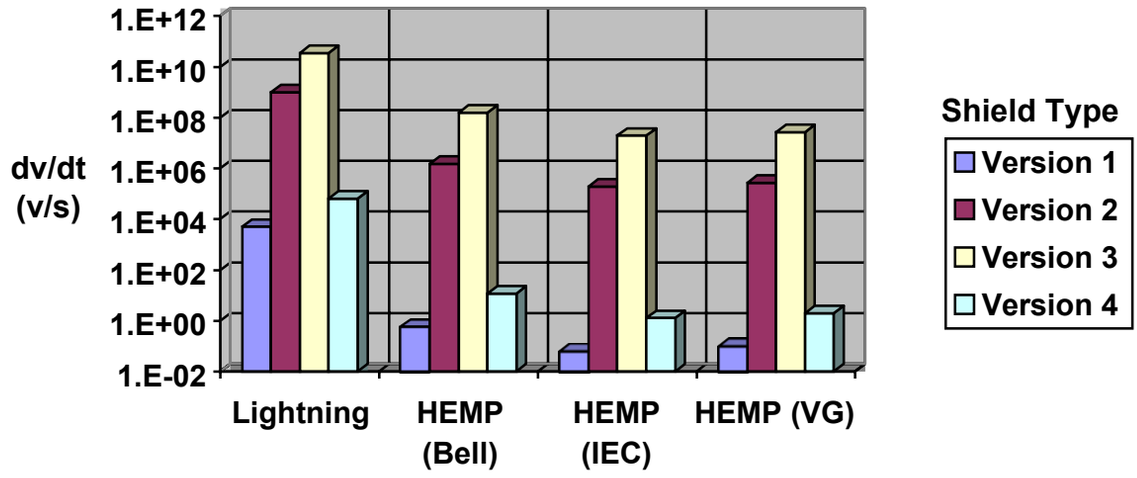

Figure 22. Plot of the 90% peak derivative of the voltage responses of the internal shielded wires as a function of the EM environment. (Line length = 1 km.)

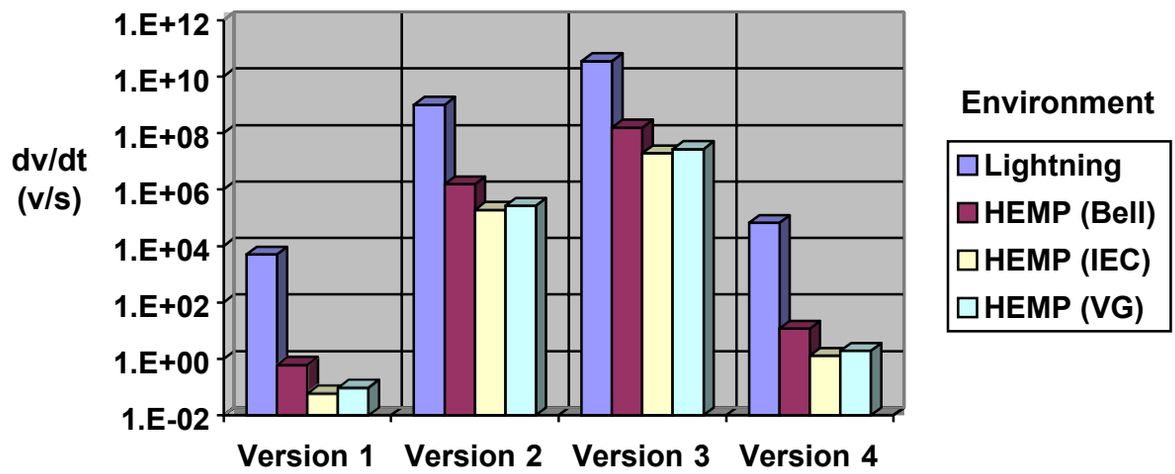

Figure 23. Plot of the 90% peak derivative of the voltage responses of the internal shielded wires as a function of the cable shield version. (Line length = 1 km.)

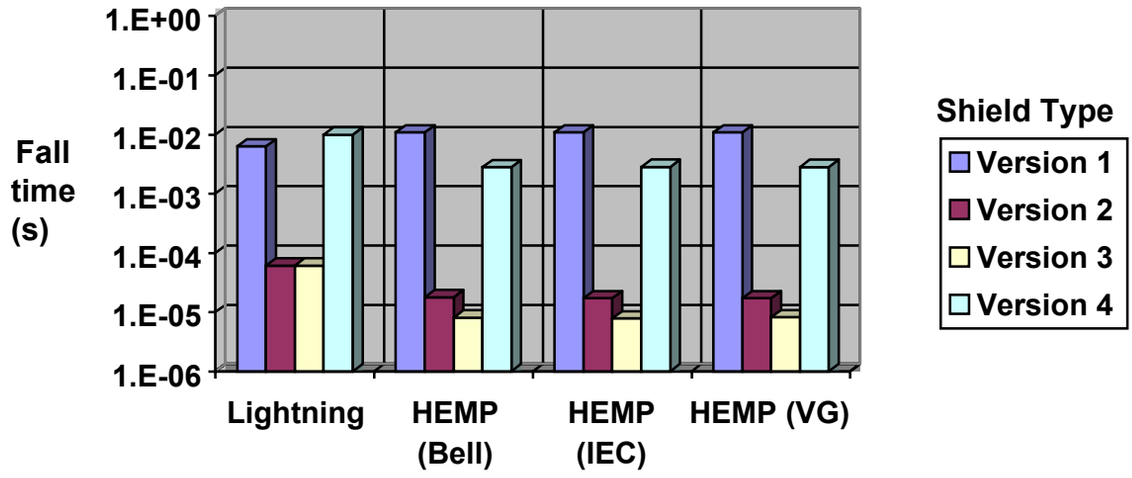

Figure 24. Plot of the 90% occurrence of the 0-50% fall time of the voltage responses of the internal shielded wires, as a function of the EM environment. (Line length = 1 km.)

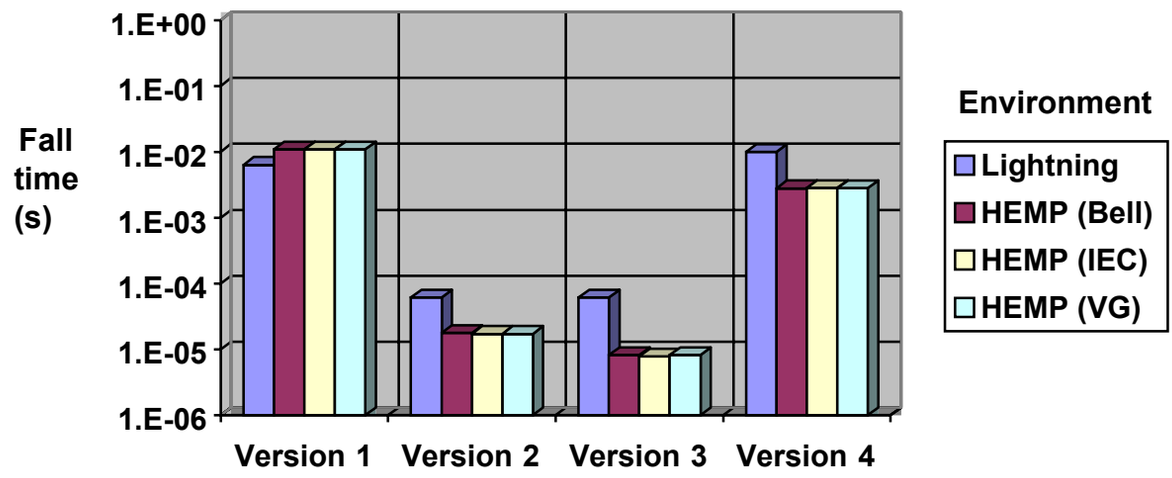

Figure 25. Plot of the 90% occurrence of the 0-50% fall time of the voltage responses of the internal shielded wires, as a function of the cable shield type. (Line length = 1 km.)

6. References

1. Tesche, F. M., "Voltage and Current Surge Characteristics for Buried and Above-Ground Cables Excited by a NEMP", Technical report submitted to the NEMP Laboratory, Spiez, October 1, 1997. A copy can be obtained from Dr. D. V. Giri by e-mailing him at Giri@DVGiri.com

2. Baum, C. E. "Electromagnetic Topology for the Analysis and Design of Complex Electromagnetic Systems," pp. 467-547 **in Fast Electrical and Optical Measurements, Vol. I**, eds. I.E. Thompson and L.H. Luessen, Martinus Nijhoff, Dordrecht, 1986.

3. Tesche, F. M., D. V. Giri and A. W. Kaelin, "Direct-Strike Lightning Response Estimates of Buried Cables within a Communications Facility", Interaction Note 630, 6 November 2019.

4. Bell Laboratories, ***EMP Engineering and Design Principles***, Technical Publications Department, Bell Laboratories, Whippany, NJ. 1975.

5. IEC 1000-2-9: "Immunity to High Altitude Nuclear Electromagnetic Pulse (HEMP): Description of the HEMP Environment, Radiated Disturbance", 1996.

6. VG 95371-10 (11-95), German Standard Environment for HEMP (text in German)

7. Tesche, F. M., et. al., **EMC Analysis Methods and Computational Models**, John Wiley and Sons, New York, December 1996.

8. Vance, E.F., **Coupling to Shielded Cables**, Krieger Press, Melbourne, FL, 1987.